

SLICE-SELECTIVE B₁ PHASE SHIMMING AT 9.4 TESLA

J. Hoffmann¹, J. Budde¹, G. Shajan¹, and R. Pohmann¹

¹High Field Magnetic Resonance Center, Max Planck Institute for Biological Cybernetics, Tuebingen, Baden-Wuerttemberg, Germany

Introduction: In human brain imaging at 9.4 Tesla, B₁⁺ field inhomogeneities are even more pronounced than at 7 Tesla due to the still shorter wavelength of the RF field in tissue. Despite the use of 16-channel microstrip coil arrays which avoid destructive interferences during signal reception, we observe total signal dropouts in axial slices at the level through the eyes and below when the array is driven in the quadrature mode. These signal voids are local areas of weak B₁⁺ magnitude, caused by destructive interferences of the electromagnetic waves that are transmitted by the single coil elements. Static B₁ phase shimming is the most straightforward approach addressing this problem since the homogenization of the excitation pattern within the head is solely based on a modification of the electromagnetic field produced by the coil, without the need for tailored excitation pulses. The total B₁⁺ field inside the head is a superposition of the fields transmitted by the individual channels:

$$|B_1^+(\vec{x})| = \left| \sum_{k=1}^{16} |B_{1,k}^+(\vec{x})| \cdot \exp[i(\Psi_k(\vec{x}) - \Theta_k)] \right| \quad [\text{Eq. 1}]$$

Here, Ψ_k denotes the position-dependent phase of the single B_{1,k}⁺ fields while Θ_k indicates global phase offset of the individual channels which can be introduced by the user in order to shape the summed field as desired. Obviously, *in situ* phase shimming requires a method to map the B₁⁺ field magnitude and phase of every channel rapidly and under stringent SAR limitations as well as a numerical algorithm that finds an adequate set of phase offsets from a multitude of possible phase configurations. Here we present a GUI-controlled phase shimming procedure that uses the B₁⁺ field estimation technique proposed by van de Moortele et al. [1] as well as a simulated annealing algorithm that quickly and reliably calculates the appropriate phases optimized for a user-defined shimming region based on a suitable optimization criterion.

Materials and Methods: Experiments were performed on a 9.4 Tesla whole-body magnet (Siemens/Magnex) with an elliptical 16-channel microstrip coil array. B₁⁺ field and phase maps for multiple slices were obtained first: A set of low flip angle axial FLASH images (e.g. TR = 100ms, TE = 4.12ms, 128x128, th = 6mm) was acquired in the desired slices by transmitting the RF power directly through only one array element at a time with a fixed phase offset. The signal from each of the 16 elements was sampled, which resulted in 256 magnitude images and the associated 256 phase images per slice. Relative single-channel field maps can be estimated from the magnitude images according to the method described in [1], while relative B₁⁺ phase maps are obtained from the raw phase images by removing the contributions that arise from the reception of the signal. This is done by calculating the phase relative to a reference channel as described in [2]. With the single relative field and phase maps available, a GUI (Fig. 1) displays a prediction of the total B₁⁺ field in a desired slice according to Eq. 1 dependent on a phase configuration of choice. Additionally, the user can define a ROI (white polygon in Fig. 1) in which a cost function, e.g. the standard deviation of the intensities of all pixels within the ROI divided by their mean value, is minimized by a simulated annealing algorithm ([3], implemented in MATLAB). In the experiment, the calculated phase offsets were applied by inserting coaxial cables of different lengths between the RF power splitter and the coil elements.

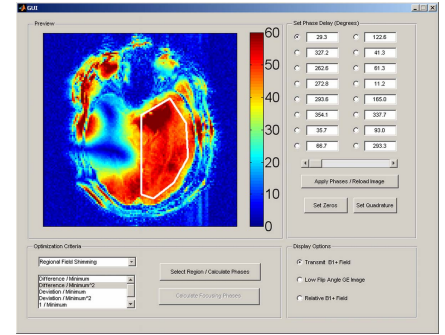


Figure 1: The GUI provides a prediction of the B₁⁺ field dependent on arbitrary phase configurations as well as the calculation of optimized configurations in user-defined ROIs.

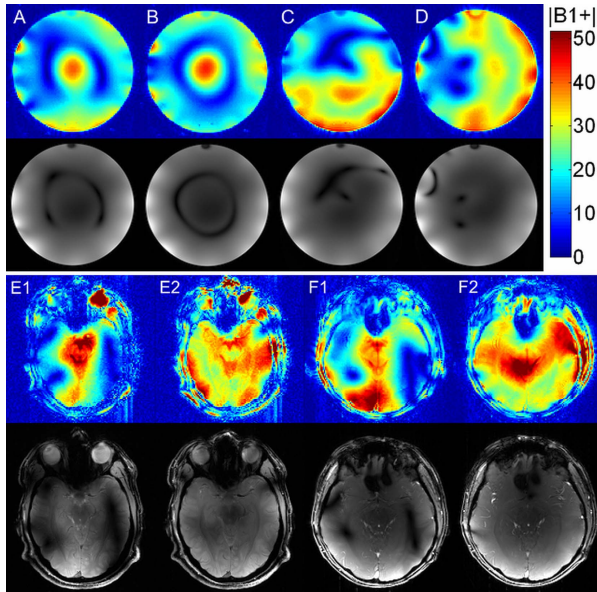


Figure 2: First row: Predicted relative B₁⁺ fields [a.u.] in quadrature (A), focused on the center (B) and shimmed to the lower (C) and right (D) half of the saline phantom. Third row: B₁⁺ field in quadrature (E1, F1) and optimized for no signal dropouts in the whole brain (E2, F2) in two different subjects. Rows two and four show the corresponding FLASH images.

Results: The field-mapping pre-scans take less than 4 minutes in total. The computational time for a set of optimized phase offsets is dependent on the number of pixels in the ROI and ranges from a few seconds up to one minute on a standard desktop computer. The first row of Fig. 2 shows predicted B₁⁺ fields for various phase configurations in a 3L saline phantom as well as the acquired FLASH images that correspond to these phase offsets (second row). The good correspondence of the signal voids in the field maps and the images demonstrates the appropriateness of the field and phase mapping method as well as the field superposition principle according to Eq. 1. Note that the FLASH images are weighted with the array sensitivity which decreases towards the center of the phantom.

B₁ shimming in axial slices approximately through the level of the eyes (where B₁ inhomogeneity is typically most severe) of two volunteers is demonstrated in the third row in Fig. 2: A ROI was drawn just along the periphery of the brain and the minimum pixel value inside the brain tissue was maximized by the algorithm. Severe signal dropouts in the quadrature mode (E1, F1) could be removed with optimized phase configurations (E2, F2). The corresponding quadrature mode and optimized FLASH images in the fourth row differ only in the phase configurations, not in the acquisition parameters.

Discussion: We demonstrated that the rapid field estimation technique [1, 2] is accurate enough to correctly predict the B₁⁺ field produced by the RF coil array across the subject. Based on this prediction, a simulated annealing algorithm can quickly calculate a set of phase offsets that optimizes the B₁⁺ field inside a user-defined ROI and according to a user-defined criterion. The GUI allows for B₁ shimming in the whole slice in order to remove signal voids (E2, F2 in Fig. 2) or to homogenize the field in smaller regions (Fig. 1). Thereby, the quality of the shim is dependent on slice position, size of the ROI and the number of coil channels. The optimization algorithm can easily be extended to perform phase and amplitude shimming if an array of RF amplifiers is available.

References: [1] Van de Moortele PF, Ugurbil K. ISMRM 2009, p.373. [2] Metzger et al. Magn Reson Med. 2008; 59:396-409. [3] Kirkpatrick S. *Science*, 220:671-680, 1983.